Annu. Rev. Fluid Mech. 2004. 36:55–79
doi: 10.1146/annurev.fluid.36.052203.071431

LANGMUIR CIRCULATION

S.A. Thorpe
Bodfryn, Glanrafon, Llangoed, Anglesey LL58 8PH, United Kingdom;
email: oss413@sos.bangor.ac.uk

Irving Langmuir (1881-1957)
Noble prize in chemistry 1932
(surface chemistry)

■ **Abstract** Since Leibovich's comprehensive review of Langmuir circulation in 1983 there have been substantial advances in modeling (notably the construction of Large Eddy Simulation models) and in observations using novel techniques that together have led to a radical change in understanding the phenomena. It is now regarded as one of the several turbulent processes driven by wind and waves in the upper layers of large bodies of water, influential in producing and maintaining the uniform surface mixed layer and in driving dispersion.

1. INTRODUCTION

In gale-force winds the appearance of lines of foam on the sea surface is used to categorize wind speed (see Table 1). But such streaks of foam or other floating material are also present in much lower winds and are almost always evident at some scale when there is material on the water surface to make patterns visible. The first scientific paper on the subject by Langmuir (1938) describes how his attention was drawn to the phenomenon when seeing Sargassum weed arrayed in linear bands during an Atlantic crossing in 1927. He realized that a local flow convergence is necessary to produce the floating bands and that conservation implies that, unless the flow in the bands increases along their extent, there must be downward motions beneath them replenished by upward flow between. He confirmed the existence of this circulation by simple but ingenious experiments performed in Lake George, NY. The circulation may be represented as an array of vortices of alternating signs with horizontal axes directed downwind, a set of Langmuir "cells" as sketched in Figure 1. Flotsam and buoyant algae accumulate in bands, called windrows, where the surface flow converges (Figures 2,3). The separation of bands at sea generally ranges from about 2 m to 1 km and their lengths are three to ten times greater. The downwind flow is greater in and below the bands than between them. Consequently, the downwind speed of floating material, carried into windrows, exceeds the mean downwind surface flow; tracking floating surface drifters carefully designed to follow the water motions may not provide a reliable means of measuring the mean speed of the water at the sea surface!

TABLE 1

Beaufort scale	Classification	Wind speed (ms^{-1})	Appearance of sea surface
7	Near Gale	13.9–17.1	Sea heaves up: white foam from breaking waves begins to be blown into streaks
8	Gale	17.2–20.7	Moderately high waves of greater length: foam is blown into well-marked streaks
9	Strong Gale	20.8–24.4	High waves: dense streaks of foam

Adapted by Peterson from the Beaufort Wind Scale devised by Admiral Sir Francis Beaufort, c.1832, and adopted by the International Meteorological Organization, 1939.

"Langmuir circulation" (Lc) is now the name commonly given to the class of motions that Langmuir was the first to investigate. It is sometimes referred to by the plural title, "Langmuir circulations." Though this aptly reminds us that, over the large range of scales and conditions in which the flow pattern is observed there may be different processes that drive similar patterns of flow, which conform to its rather loose definition, I shall retain use of the singular case.

Discovering the causes of Lc and quantifying and identifying its effects has been difficult. Studying the associated dynamical processes involves some of the most

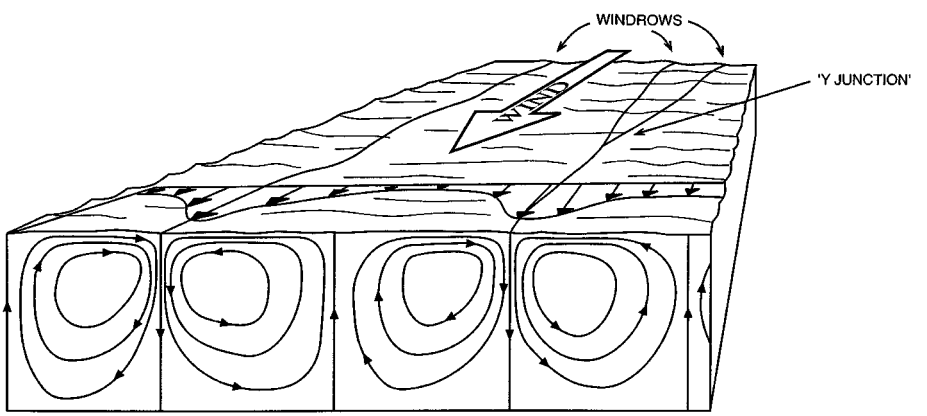

Figure 1 Sketch showing the pattern of mean flow in idealized Langmuir circulation. The windrows may be 2 m to 300 m apart, and the cell form is roughly square (as shown). In practice the flow is turbulent, especially near the water surface, and the windrows (Figure 2) amalgamate and meander in space and time. Bands of bubbles or buoyant algae may form within the downward-going (or downwelling) flow (see Figure 3).

intellectually demanding problems of theoretical and observational fluid dynamics, several of which remain intractable. Among them are the instability and growth of both small and finite disturbances in unsteady flow [even the formulation of the equations of motion demands meticulous care in correctly averaging over many wave periods (Leibovich 1977)]; the interaction of large coherent eddies with wave- and shear-generated turbulence near the free surface and with internal waves in the stratified, underlying thermocline; and the effect of (unsteady) circulation on the dispersal of neutral or buoyant, even motile, particles (bubbles, oil, and plankton). Scientific understanding of Lc has undergone substantial advance and change within the last two decades. At the time of Pollard's (1977) and Leibovich's (1983) reviews the main objective of study was to explain how the circulation is produced. Although attention had been drawn earlier to its effect on dispersion (Csanady 1973), Lc was usually regarded as regular and steady, apparently constraining lateral dispersion by carrying material into narrow bands and inhibiting, rather than enhancing, dispersion.

This perspective has now changed, partly because of developments in numerical simulation, particularly Large Eddy Simulation (LES) models (Skyllingstad & Denbo 1995, McWilliams et al. 1997), but mainly as a result of new methods of observation, notably sidescan Doppler sonar (Smith et al. 1987) and freely drifting instruments (Farmer & Li 1995), or automated underwater vehicles (AUVs) (Thorpe et al. 2003a). Although Lc produces bands that are generally orientated downwind, they are rarely steady, linear, or regularly spaced, but are more often twisted and subject to amalgamation one with another (Figure 4). Lc is now regarded as one of the several turbulent processes that operate in the upper boundary layers of oceans and lakes, contributing substantially to the dispersion of floating material such as oil (Figure 5). Lc complements, interacts with, and often dominates other turbulent processes that transport momentum and heat or that drive dispersion in the upper ocean. However, in spite of its evident importance, Lc is not presently represented or parametrized in global circulation and climate models, or even in smaller scale models used to predict dispersion of oil spills (D'Asaro 2000).

Although I shall refer to work before 1983, most is fully described in the earlier reviews. My main purpose is to explain how the perspective changed, describe subsequent developments, and identify where knowledge is still lacking. For ease of presentation, and because the legacy of earlier work left outstanding some problems that underpin and provide context to the later developments, I shall follow the conventional trail of describing the several factors that affect Lc (Section 4) before discussing its instability and variability, and the insight given by LES models (Section 5). Although this inevitably results in referring to some things before they are fully described, I leave the description of observations of Lc until Section 6. In Section 7 I briefly discuss the consequences of Lc in large water bodies, the oceans, lakes, or reservoirs. I request the patience of the reader where disorder is apparent and irritating, and apologize for what, through lack of space, is omitted.

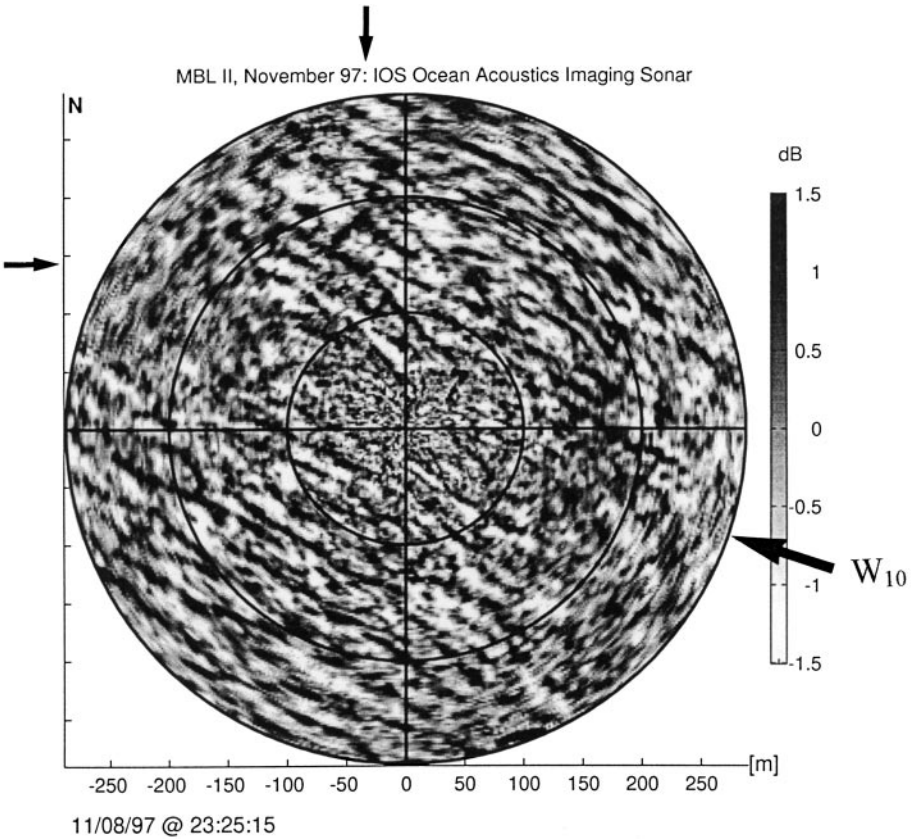

Figure 4 Rotating sidescan image of bubble clouds (*dark bands*) below the sea surface to a range of about 300 m from the 100-kHz sonar (*center*) hanging 30 m below the water surface and supported by a surface float. The wind, W_{10}, (*arrow*) is 13 ± 1 ms^{-1}. Small arrows show the coordinates of a Y junction. (Kindly provided by Professor D.M. Farmer. See also Farmer et al. 2001.)

2. LANGMUIR CIRCULATION AT THE ONSET OF WIND

Bands at 2–10-cm spacing occur shortly after the onset of wind and have been known for some time (e.g., Faller & Caponi 1978, Kenney 1993), but only recently have detailed laboratory and field studies been made (Veron & Melville 2001, Handler et al. 2001). The onset of Lc in a previously quiescent fluid occurs at Re $= 530 \pm 20$ and after the first appearance of surface waves at Re $= 370 \pm 10$, where Re $= U_0(\nu t)^{1/2}/\nu$, U_0 is the surface water speed, ν the kinematic viscosity, and t the time after the onset of wind. The wavelength of the instability is of order $150\nu/u$, where $u^2 = \nu[U_0/(\nu t)^{1/2}]$ is a measure of the surface stress at the onset

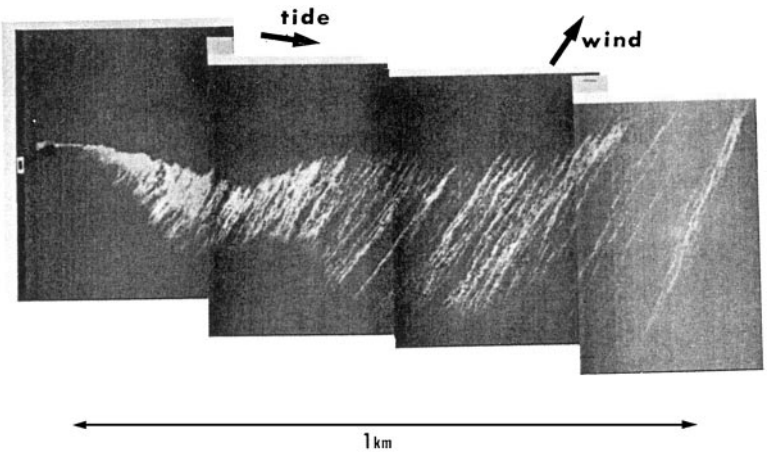

Figure 5 Spread of oil carried by a tidal flow from a fixed source at the left of the picture, a composite of infrared images taken from an aircraft. The Lc draws the oil into bands in the wind direction. The wind speed is about 10 ms^{-1}. (Images kindly provided by Dr. T. Lunel.)

of instability. The circulation is a factor in air-sea fluxes in low winds, is visible in infrared images of surface temperature (Figure 6), and affects the structure, stability, and transports across the cool skin of the ocean. Numerical studies by Handler et al. (2001) that exclude both buoyancy and surface waves show that this instability is caused by viscous shear at the free surface and not by waves or thermal convection, unlike the instability and Lc described in following sections.

3. PARAMETERS, SCALES, AND EQUATIONS OF MOTION

Although other factors (described below) may be influential, it is now widely accepted that what is usually identified as Lc at scales of 2 m–1 km on sea or lake surfaces (and to which scales the remainder of this review is directed) generally arises through the interaction of the Stokes drift induced by surface waves and the vertical shear in turbulent fluid, consequently producing a vortex force as described by the so-called CL2 model of Craik & Leibovich (1976). The instability may be explained physically by supposing that a small spanwise perturbation occurs in a uniform downwind Stokes drift and shear flow. This perturbation necessarily involves the presence of a vertical component of vorticity, and consequently introduces a horizontal vortex force directed towards the plane of the maximum flow perturbation. Therefore, there is an acceleration of fluid towards this plane where (neglecting downwind variation) continuity implies that the flow must sink, leading to a circulation with downwind vorticity. Kinematically, the

vertical gradient of Stokes drift tilts the vertical vortex lines resulting from the spanwise perturbation, creating streamwise vorticity. So far this disregards the frictional effects of small-scale turbulence that may dampen or assist the motion. Downwind flow in the convergence region, enhancing the original perturbation and providing feedback, is a consequence of acceleration caused by the stress of the wind on water particles as they move at the surface from the upwelling to the convergence region, perhaps affected by changes in turbulent drag near the downwelling site (Li & Garrett 1993). The generation process depends critically on the Stokes drift induced by surface waves and is consequently distinct from the processes that drive rolls in the atmospheric boundary layer (e.g., see Etling & Brown 1993).

The process may be formulated as one in which the flow averaged over the wave field is forced by a wind stress, τ, characterized by a friction velocity, $u_* = \sqrt{(\tau/\rho)}$, where ρ is the density of water, and a Stokes drift, $u_s = 2S_0 e^{2\beta z}$. Except in LES models (Section 5) it is customary to represent small-scale turbulence by an eddy viscosity, v_T. In the absence of stratification or surface heat flux, and if the wind stress and Stokes drift are parallel and both in the x-direction, the spatially averaged, nondimensionalized equations of motion become

$$\partial u/\partial t + v\partial u/\partial y + w\partial u/\partial z = La\nabla^2 u, \tag{1}$$

$$\partial \Omega/\partial t + v\partial \Omega/\partial y + w\partial \Omega/\partial z = La\nabla^2 \Omega - (du_s/dz)(\partial u/\partial y), \tag{2}$$

with $v = -\partial\psi/\partial z$, $w = \partial\psi/\partial y$, and the vorticity, $\Omega = \nabla^2\psi$, where ψ is a stream function. Following Li & Garrett (1997), and assuming v_T does not depend on depth, z, the transverse (y) and vertical (z) lengths have been nondimensionalized by β^{-1}, the time, t, by the evolution time scale, $(\nu_T/u_*^2)(\nu_T S_0\beta/u_*^2)^{-1/2}$, the downwind x-component of velocity, u, by $u_*^2/\nu_T\beta$, and the vertical and transverse (y) velocity components (w and v, respectively) by $(u_*^2/\nu_T\beta)(\nu_T S_0\beta/u_*^2)^{1/2}$. The surface boundary conditions are

$$\partial u/\partial z = 1 \quad \text{and} \quad \Psi = \nabla^2\Psi = 0 \quad \text{at} \quad z = 0. \tag{3}$$

The flow is determined by the Langmuir number, La, defined as

$$La = (\nu_T\beta/u^*)^{3/2}(S_0/u^*)^{-1/2}, \tag{4}$$

which expresses a balance between the rates of diffusion of downwind vorticity and its production by vortex tilting and stretching by the effect of Stokes drift. (The definition, $La = (\nu_T^3 k^2/\sigma a^2 u_*^2)^{1/2}$, adopted by Leibovich (1983), applies directly to monochromatic waves with amplitude, a, and frequency, σ, and wavenumber, k. For such waves, $u_s = a^2 k\sigma e^{-2kz}$, so S_0 becomes $a^2\sigma k/2$, and Leibovich's La, with $\beta = k$, is $2^{-1/2}$ times that defined in Equation 4.)

Estimating the size of La in the ocean requires some means to find S_0, u_* and β. From the empirical Pierson-Moskowitz spectrum of surface waves,

$$2S_0 = (0.014 \text{ to } 0.015)\, W_{10}, \tag{5}$$

and u_* lies in the range (1.05 to 1.54) $\times 10^{-3}\, W_{10}$, and

$$\beta^{-1} = 0.24\, W_{10}^2/g, \tag{6}$$

where W_{10} is the wind speed at the standard height of 10 m above the water surface and g is the acceleration due to gravity (Li & Garrett 1993). Using values of ν_T derived from observations (Huang 1979), oceanic values of La are typically of order 0.01.

Other factors affect the developing circulation. Buoyancy effects may be caused by heat loss at a rate, Q, per unit surface area from the water surface, or by stratification with buoyancy frequency, N (usually assumed constant). The temperature, θ, then varies according to the heat conservation equation

$$\partial\theta/\partial t + v\partial\theta/\partial y + w\partial\theta/\partial z = LaPr^{-1}\nabla^2\theta, \tag{7}$$

and a buoyancy torque term $H_0 Pr\partial\theta/\partial y$ must be added to the right hand side (r.h.s.) of (2), where temperature has been nondimensionalized by $Q/c_p\rho\kappa_T\beta$ when the water surface loses heat at a rate, Q, or by $N^2/\alpha g\beta$ when the water column is vertically stratified. The surface boundary condition for heat flux is $\partial\theta/\partial z = -1$, or $\theta = 0$ in the stratified case when the surface temperature is held constant. There are now two further parameters. The Prandtl number is

$$Pr = \nu_T/\kappa_T, \tag{8}$$

expressing the relative importance of momentum and heat diffusion, where κ_T is the eddy diffusivity of heat. (It is often assumed that Pr is equal to 1.) For a surface heat flux, Q, the Hoenikker number is

$$H_0 = (\alpha gQ/c_p\rho)/S_0\beta u_*^2, \tag{9}$$

which may be written as $H_0 = (4/\kappa)(2S_0/u_*)(2\beta L)^{-1}$ in terms of $L = -u_*^3/\kappa B_0$, the Monin-Obukov length scale. κ is von Karman's constant, approximately equal to 0.41, and $B_0 = -\alpha gQ/c_p\rho$ is the surface buoyancy flux, neglecting the effect of surface evaporation that may lead to (usually small) changes in salinity. For winds of 10 ms^{-1} and a surface heat loss of 200 Wm^{-2}, H_0 is about 0.014, but surface heating leads to values of H_0 between -0.1 and 0 (Li & Garrett 1995). Alternatively, for a stratified water column,

$$H_0 = 4N^2/(U_s' U'), \tag{10}$$

where $U_s' = 4S_0\beta$ is the vertical gradient of the Stokes drift at the surface and $U' = u_*^2/\nu_T$ is the vertical gradient of the mean Eulerian current at the surface. $H_0 Pr$ represents the ratio of convective or buoyancy forcing to that of the vortex force associated with surface waves. The effect of the Earth's rotation is a further factor that may have substantial effects, as Section 4 shows.

4. PROCESSES AFFECTING LANGMUIR CIRCULATION

Leibovich & Paolucci (1981) found that a homogeneous flow is unstable to two-dimensional (2D) rolls if La < 0.47. Because La ~ 0.01 in the ocean, the instability leading to the vortical structure of Lc is at least possible there. Whether or how it actually occurs depends on the development to finite amplitude and on the nature or changes in the forcing. Leibovich (1983) mentions several processes that may affect whether or not Lc occurs, among them thermal convection, surface films, surface stresses caused by roll vortices in the atmosphere and Ekman layer instability, and he gives reasons for discounting their major importance. Some factors affecting Lc were reexamined in recent years by solving the equations described in Section 3; the conclusions of these investigations are described below.

Surface Cooling and Heating; Stratification

Li & Garrett (1995) use a numerical method to solve the above equations when there is a surface heat flux. Stratification induced by strong surface heating can suppress or even inhibit Lc, but in the likely parameter range of small La and $-0.1 <$ Ho < 0 at sea, the effects of heating are relatively small. (However, Lc can be completely inhibited at some value of H_0 between -2 and -4.) Convection resulting from surface cooling will also likely have little effect. In the range $0.01 <$ La < 0.2, convective forcing only dominates over that ascribed to the effect of wave-driven Stokes drift if $H_0 > 1$, rare in the ocean. Variation of Pr from 0.5 to 2 has little effect on the speed of downward or downwind flow for realistic values of La. Therefore, the CL2 mechanism generally dominates over thermal convection in driving Lc in the ocean. Gnanadesikan (1996) reaches a similar conclusion using a Mellor-Yamada 2 1/2-level turbulence closure model with constant ν_T.

Li & Garrett (1997) study the formation of an oceanic mixed layer by Lc. They model the effect of imposing a surface wind stress on initially stationary water, maintaining a uniform stratification with buoyancy frequency, N, by imposing a constant surface heat flux. Two alternative conditions for mixed layer deepening are formulated in terms of Δb, the fractional change in buoyancy ($g\Delta\rho/\rho$) between the bottom of the mixed layer and the top of the thermocline. The first is derived from a bulk Richardson number criterion similar to that of Price et al. (1986):

$$\Delta b \geq 0.65|\Delta u|^2/h, \tag{11}$$

where $|\Delta u|$ is the difference in speeds at the same location, often driven largely by inertial motions, and h is the mixed layer depth. The second is based on the engulfment of stratified water in the mixed layer as a consequence of Lc:

$$\Delta b \geq 50u_*^2/h. \tag{12}$$

The coefficients are derived from a numerical model. Li et al. (1995) critically apply these conditions to data to determine whether Lc or inertial shear drives the deepening of mixed layers (Price et al. 1986). Some periods, but not all, are

found in which the observed deepening cannot be attributed to shear and seem most likely a consequence of Lc.

In reassessing the stability of a stratified flow with constant buoyancy frequency, N, Phillips (2001) shows that although the inviscid flow is linearly stable if

$$N^2 > U_s' U', \tag{13}$$

(Leibovich 1977; similar to a Richardson number criterion), viscosity may mildly destabilize the flow at very low La but beyond the range of La common in the ocean. Decrease in Pr tends to destabilize the flow. Phillips suggests that this result helps to explain Smith's (1992) observation (see Section 6) of an apparent onset of Lc after an increase of wind (because it is not certain that the scale of Lc bands could be properly resolved before the increase) even though the value of La hardly changed, arguing that Pr may have decreased with enhanced turbulence. Phillips also examines the effect of introducing realistic profiles of the mean shear flow and of the Stokes drift, finding that these may decrease the critical value of La by a factor of order 10.

The Earth's Rotation

The vertical structure of the mean current and shear observed in the near-surface mixed layer is not replicated in slab models (e.g., Price et al. 1986) or by Meller-Yamada level 2 turbulence closure models. This prompted Gnanadesikan & Weller (1995) to examine the stability of an Ekman layer flow in the presence of an infinite train of surface gravity waves. Although finding that the orientation of roll vortices shifted to the right of the wind in the northern hemisphere as a result of the Ekman shear in accordance with Faller's observations (1964), their results support the hypothesis that Lc in the ocean is primarily driven by wave-current interaction rather than by Ekman or shear instability. The Ekman spiral predicted on the assumption of small-scale turbulent mixing frequently led to highly unstable conditions, and the resultant mixing over the depth of the layer by Lc replaced the small-scale mixing as the primary mechanism in the vertical transport of momentum and heat. However, the analysis is not entirely consistent with observations. It found that surface waves induce an Eulerian return flow, which is not observed, to balance their Stokes drift transport, and only large cells with scales typically 200 m are predicted, whereas there are smaller scales in the ocean.

The Effect of Wave Groups and Breakers

Gnanadesikan & Weller (1995) raise an interesting point relating to their assumption of an infinite surface wave field. In practice, the wave field often has a group-like structure. McIntyre (1981) points out that wave-induced Stokes drift, and a return flow, should be locally confined to a wave group. Great care is needed in making assumptions of spatial uniformity of the wave-averaged Eulerian and Lagrangian flow fields and in deriving the equations of motion. Wave groups may have other consequences, such as causing wave breaking to reoccur with a

period of approximately twice the wave period (Donelan et al. 1972). The effect of wave breaking on Lc has hardly been addressed, although both Csanady (1994) and Teixeira & Belcher (2002) suggested the possibility that breakers provide the (finite amplitude) perturbations that initiate Lc, or that Lc is "seeded" through the vorticity produced by breaking waves.

Variable Forcing

An important direction of recent research is studying the effect of the unsteady wind forcing typical of natural conditions. Changes in wind speed lead to temporal variation in wave amplitude. This results in a z-component of Stokes drift that leads to an addition forcing term in Equation 2, contributing to the streamwise vorticity that in a sense depends on whether waves are growing or decaying. Under physically severe restrictions on the forcing parameters that allow terms to be separable and the problem tractable, Phillips (2002) concludes that, in general and relative to steady conditions, wave growth reduces the likelihood of Lc by increasing the value of La for its onset, whereas wave decay correspondingly enhances the formation of Lc for sufficiently large-scale cells.

Because of variations in wind direction and the relatively slow adjustment of the wave field, the Stokes drift and the wind stress are not always aligned in the same direction. The orientation and fastest growth of Lc depend on the angle φ between the two. For a given φ, the fastest growing circulations occur when the direction of the Lc vortices lies between those of the Stokes drift and the wind (Polonichko 1997, Cox 1997). The direction depends on both φ and the shear ratio $\mathrm{Sr} = \mathrm{U_s^{/}/U^{/}}$. The growth rate is greatest when $\varphi = 0$ and decreases with increasing φ. When $\mathrm{Sr} < -0.5$, the orientation of the Langmuir vortices is also sensitive to the shear gradient parameter $\mathrm{Su} = \mathrm{S_0/u_*}$. However, these results do not provide information about a finite amplitude steady state, if one exists. They also assume that the wind stress and wind are aligned, which may not always be the case (see Rieder & Smith 1994), and they ignore the (possibly developing) drift and rotational motions associated with Ekman flow.

Interactions with Internal Waves

Internal waves in the thermocline can affect Lc in several ways. Thorpe (1997) suggests that Langmuir cells may be twisted and stretched if the line of the internal wave crests is not parallel to the Langmuir vortices, leading to enhanced vorticity. The phase speed of internal waves traveling in directions normal to the vortices (i.e., in the y-direction) is reduced by interacting with Lc. Chini & Leibovich's (2003a) recent theoretical studies confirm the reduction in phase speed, and show that internal waves of wavelength twice that of the Lc (i.e., equal to four cell widths) are reflected in much the same way as are surface waves traveling over sand bars. Chini & Leibovich (2003b) found that Lc can transfer energy to standing internal waves in the thermocline with nodes that are vertically aligned with the Lc regions of downwelling. A cycle of energy exchange between Lc and standing internal

waves leads to variations in the strength and phase of the circulation, possibly contributing to the vacillations in Lc observed by Smith (1998) (see Section 6).

5. INSTABILITY OF LANGMUIR CIRCULATION

Studies of the Cause of Instability

By the early 1990s, observations had demonstrated the transient and variable nature of Lc. Theoretical study was at first simplistic. Thorpe (1992) examined the stability of an inviscid array of vortices representing Lc, finding that vortex pairing, rather than a collective instability, was the most likely form of instability. Li & Garrett (1993) devised a 2D model to examine the merging of neighboring Langmuir cells. Although they found that cells merge only when forced by the presence of Stokes drift, the relevance of their results are questionable in view of the observed importance of three-dimensionality in the merger of vortices, such as that of contrails (Crow 1970).

Tandon & Leibovich (1995a,b) show that even in the greatly simplified conditions of an unstratified fluid of depth, d, with nonslip bottom, uniform Stokes drift gradient and constant ν_T, a variety of unstable modes of instability may evolve, depending on the size of two parameters, a Reynolds number $Re = u_* d/\nu_T$, and a Rayleigh-like parameter, $R = Re^2 Rs_s$ $(= (2La)^{-1})$, where $Re_s = 2S_0 d/\nu_T$ is the Reynolds number of the Stokes drift. Rolls are possible only when $R > R_c = 669.0$. Computations of the finite amplitude nonlinear instability of steady Langmuir rolls at particular parameter values show that at $Re = 22.4$ a sinuous traveling wave mode propagating in the downwind direction sets in at $R > 725$, and this is subject to vacillations at $R > 900$. At $Re = 5.9$, traveling waves occur above a value of R between $8R_c$ and $15R_c$.

In reality, a rich set of different instabilities may exist. In winds >12 ms^{-1}, Farmer & Li (1995) observe that pairs of bands amalgamate into one in Y junctions (see Figures 1 and 4), predominantly pointing downwind with an angle between the pair at the junction of about 30°. Bhaskaran & Leibovich (2002) explain these features using a model that includes the Earth's rotation. The Y junctions appear as defects at locations where the real and imaginary parts of an amplitude function are both zero.

LES Models

A major difficulty in comparing theory based on the equations of Section 3 with observations is that of appropriately choosing the turbulent eddy viscosity, ν_T. This is particularly acute because values estimated from sea-going experiments (Huang 1979) naturally include the effects of existing Lc. The numerical LES models of Lc formulated by Skyllingstad & Denbo (1995) and McWilliams et al. (1997) avoid the necessity to assume an a priori form for ν_T and, unlike earlier models, include three-dimensionality. They clarify that the eddy viscosity is an internal

parameter, determined by the turbulent motions, including Lc, and not one that should be imposed ad hoc. McWilliams et al. defined a new parameter referred to as a "turbulent Langmuir number,"

$$La_{turb} = (u_*/2S_0)^{1/2}, \quad (14)$$

with values typically about 0.3 in the ocean. The advantage is that it can be estimated from observations, so allowing comparison with predictions, unlike La.

The LES models are successful in reproducing many of Lc's observed features, most notably its unsteadiness, the tendency for cells to have a nonuniform distribution in size, to amalgamate with Y junctions pointing downwind, and to draw floating particles into linear bands (see Figure 7). Both sets of authors include the effects of the Earth's rotation, although results differ slightly because Skyllingstad & Denbo omitted a Coriolis vortex force due to the Stokes drift.

Skyllingstad & Denbo examined the initial growth of cells and found that although the early development is similar to that described by 2D theory, the pattern soon breaks down with three-dimensional (3D) interactions between cells. The consequences of separately adding the effects of turbulent motions driven by heating and cooling, wind stress, and Stokes drift demonstrate the importance of Lc in generating circulation and linear patterns of floating material, and show that within a range $-0.188 < \mathrm{Ho} < 0.058$, Lc is more important than convection in deepening the mixed layer, in accord with Li et al. (1995). The longitudinal to transverse aspect ratio of active coherent cells of about 3–4 found in the models is smaller than those generally estimated from observing bubble clouds or windrows. McWilliams et al. used conditional sampling to describe the structure of Lc. The scale and nature of coherent patterns changed with depth (Figure 8); the relatively small-scale downwind linear patterns near the surface were replaced at depths beyond the e-folding scale of the Stokes drift by larger-scale features inclined to the wind (an aspect that deserves observational verification).

Whereas Lc enhances turbulence near the surface to levels above those predicted by the Law of the Wall relation or expected in convective motions, the present LES models of Lc do not represent breaking waves or the localized production of vorticity and turbulence (McWilliams & Sullivan 2000). They are consequently most uncertain in the depth range where the effect of Lc on the turbulent field is greatest (although also where observations are few and most difficult). It is possible that one can rectify this deficiency in models following the recent developments of Large Wave Simulations (LWS) (see Dimas & Fialkowski 2000).

6. OBSERVATIONS

The Scale and Structure of Lc

Windrows and bubble bands show a hierarchy of separation scales (twice the Langmuir cell widths) with average values that increase slowly with wind speed

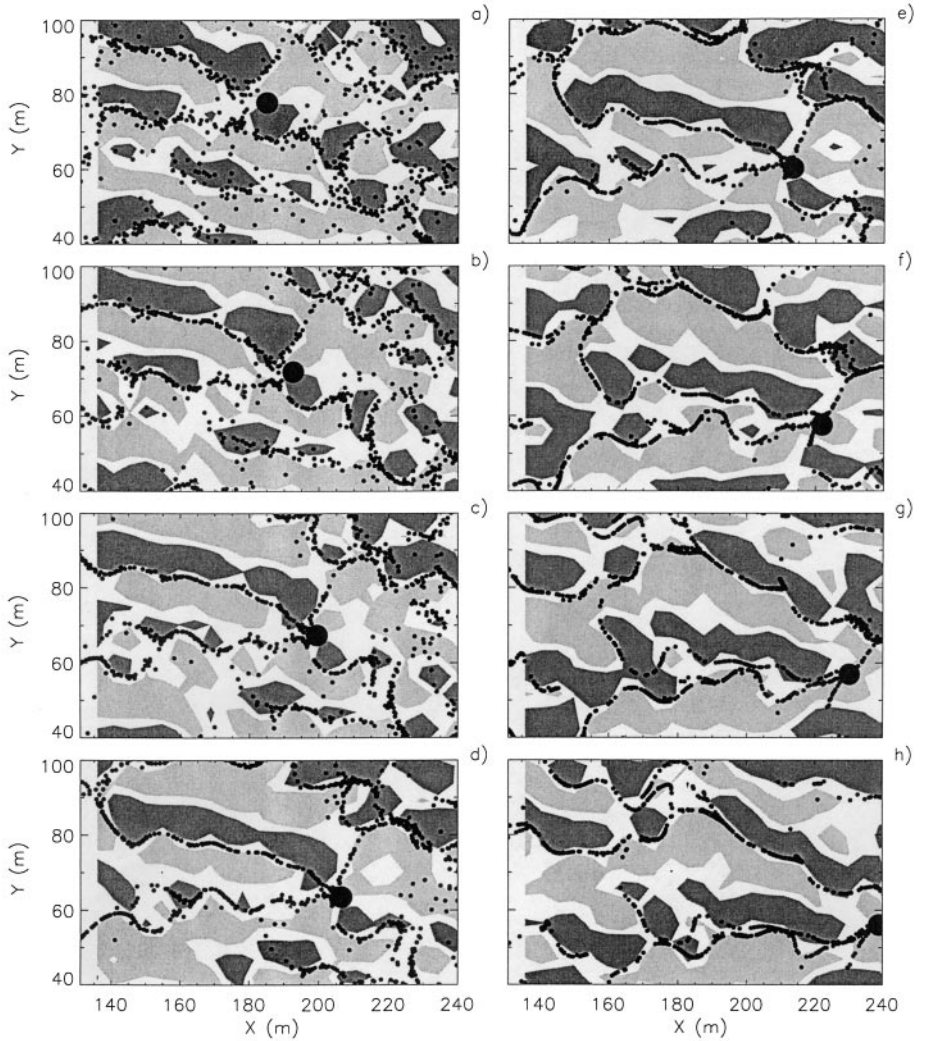

Figure 7 A Large Eddy Simulation of the dispersion of floating particles. The shaded areas are vorticity contours in the wind direction at a depth of 1.8 m, dark $>0.0055\ s^{-1}$ and light $<0.0055\ s^{-1}$. Dots indicate particles. Parts a–h are at times 288, 448, 576, 704, 832, 992, 1120, and 1248 s, respectively, after particles were released randomly across the x–y domain. The large circular black dot marks the location of a particle near a developing Y junction. Cell merger occurs to the left of this particle. (From McWilliams et al. 1997, with kind permission of Cambridge Univ. Press.)

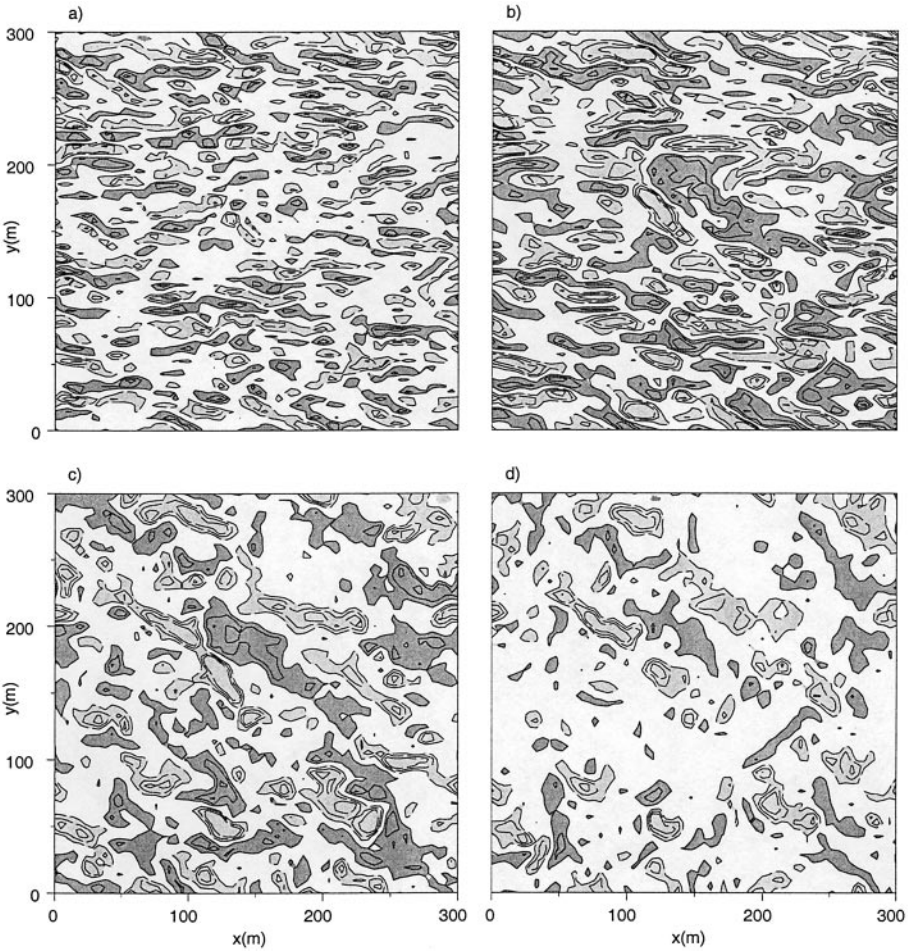

Figure 8 Contour plots of vertical velocity on horizontal surfaces at depths of (*a*) 0–3, (*b*) 3–12, (*c*) 12–20, and (*d*) 20–30 m, derived from a Large Eddy Simulation model including surface cooling and rotation. Dark shading marks downward flow >0.005 ms^{-1} and light shading shows upward motions >0.005 ms^{-1}. Wind-aligned, x-directed, linear features at smaller depths in (*a*) are replaced at greater depth by larger scale features aligned across wind, (*c*). The mixed layer depth is 33 m, $La_{turb} = 0.3$, $L = -240$ m, and $\beta = 0.0105$ m^{-1}. (From McWilliams et al. 1997, with kind permission of Cambridge Univ. Press.)

(Thorpe et al. 1994, Farmer & Li 1995) and with log normal pdfs, which Csanady (1994) suggests is due to forcing the LC2 instability by breaking waves. Band lengths also increase with wind and have approximately lognormal pdfs (Farmer & Li 1995).

Weller et al. (1985) and Weller & Price (1988) made careful and detailed observations from the floating instrument platform (FLIP) using vertical profilers and vector measuring current meters, demonstrating the related vertical and downwind flows beneath prominent windrows (Figure 9). Backscatter intensity sonar or sidescan sonar, and Doppler sonar, have also proved powerful tools to observe Lc. For example, Zedel & Farmer (1991) demonstrate the relationship between the horizontal pattern of bubble bands detected by sidescan sonar and the downward penetrating bubble clouds viewed by a vertically pointing beam (Figure 10). Doppler sonar provides the means to record the pattern of convergent and divergent surface flow in Lc in range and time (Plueddemann et al. 1996) (see Figure 11).

If the e-folding scale β of the Stokes drift is proportional to the wavelength of the dominant waves, λ, the scale of the cross-wind surface velocity becomes

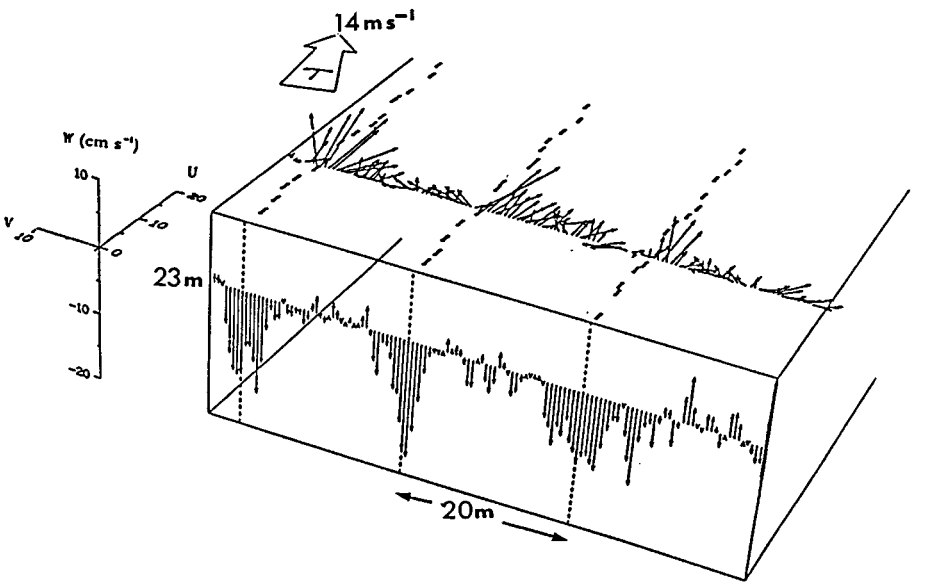

Figure 9 Currents in Langmuir circulation. A three-dimensional presentation of a time series of data taken from (FLIP) showing the vertical currents, W, measured at 23-m depth and horizontal current vectors (U, V, also at 23-m depth) beneath (*dashed*) windrows detected by scattering computer cards. The distance, 20 m, is an approximate indication of windrow separation. (From Weller et al. 1985 with kind permission of American Association for the Advancement of Science.)

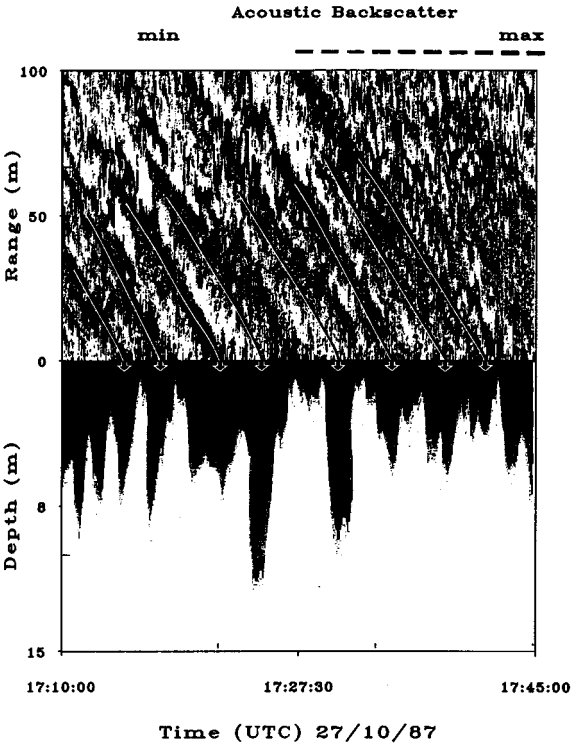

Figure 10 Bubble bands. Simultaneous sidescan (*top*: scale is "range" along the sea surface) and upwards pointing sonar (*below*: scale is "depth") images, dark areas showing bubble clouds. A period of 35 minutes is shown with the instrument drifting through bands of bubble, deeper clouds are generally detected as the bands pass. Lines (*white*) are drawn to aid identification of the bands. (From Zedel & Farmer 1991.)

$V_{CL} = u_*(\lambda S_0/v_e)^{1/2}$ (see Section 3). Plueddemann et al. suggest that $v_e \sim \lambda u_*$ giving $V_{CL} \sim (u_* U_s)^{1/2}$, which aligns with their observations. However, by confining data to those in which Lc bands are visible in Doppler sonar, Smith (1998) finds that the optimal fit is $V_{CL} \sim U_s$, once Langmuir circulation is established, but with a presently unknown proportionality factor that may depend on mixed layer depth or bubble void fraction.

There is conflicting evidence about the importance of Lc in driving vertical currents within the flow field of the mixed layer. Weller et al. (1985) find downwelling flows where surface drifters converge quickly into lines. Smith's (1998) observations using Doppler sonar however imply that bands of bubbles may not all be associated with active convergence. Not only may the lines of bubbles and surface velocity variation have different separation length scales because the bubble lines are closer together, but even different orientation! Perhaps a proportion of the bubble clouds are "fossil" remains of previously active bands? There is considerable

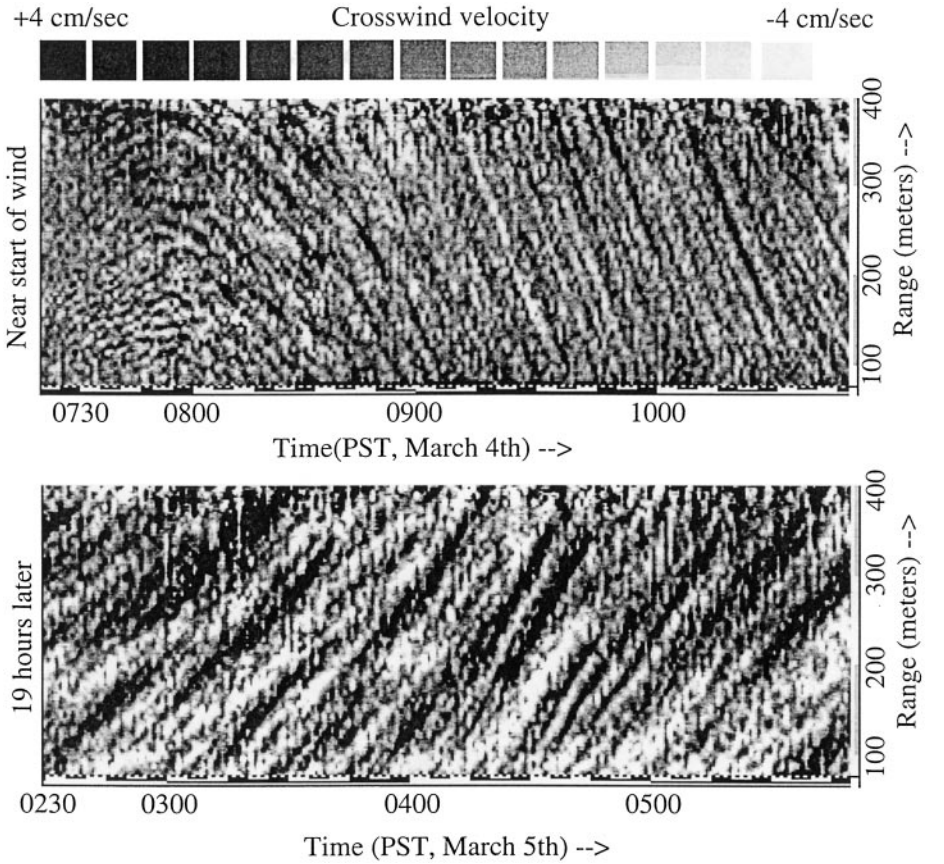

Figure 11 Near-surface convergence speed measured by Doppler sonar pointing approximately across wind. The wind increased rapidly at time = 0730 (*top*), leading to the development of a pattern of cells with gradually increasing scales that slowly drift towards the sonar. Nineteen hours later (*bottom*) the patterns show stronger flows and larger cell sizes moving away from the sonar. The near-vertical bands are caused by surface waves. (From Smith 1996.)

scatter in the downwelling speeds measured beneath windrows (Weller et al. 1985), with the range at any given wind speed almost equal to the mean. Weller & Price (1988) attribute this to the heirarchy of scales in the convergent flow patterns and a possible corresponding range of downwelling speeds. Attempts to identify motions below the water surface as Lc using Lagrangian tracking (D'Asaro et al. 1996) have not provided clear evidence for the presence of circulatory flows. The subsurface motions appear transient and variable. The ratio, σ_w/u_*, of the root mean square vertical velocity, σ_w, (excluding contributions from surface waves) to friction velocity is in the range of 1.22–1.73 (D'Asaro & Dairiki 1997)—much

larger than the values of unity or less found below a solid plane boundary. The observed ratio, σ_w/u_*, is substantially greater than Li & Garrett's (1993) 2D model predicted, but it overlaps the range predicted by 3D LES models. σ_w does not scale with the Stokes drift, S_0, as might be expected if Lc strongly affects the vertical motion field (D'Asaro 2001), but perhaps the scaling is masked in a manner similar to that found by Smith for V_{CL}.

The Growth/Onset/Decay of Lc and Vacillations

Smith (1992) describes the onset and growth of Lc following a sudden increase of wind from 8 to 13 ms^{-1}. The mean separation of bands increases at a rate about twice that of the mixing layer depth, indicating a near-constant cell width-to-depth ratio of about unity. Bravely attempts to relate the observations to the then existing theoretical predictions but is thwarted by uncertainty in estimating La and other parameters. [In reference to his expression of difficulties, Phillips (2001), refers to 'Smith's lament'!].

Smith (1998) later reports a two-hour period of relatively steady wind and wave conditions in which the Lc structure revealed by Doppler sonar varies over periods of 15 minutes between weak disorganized features and well-defined regular bands. He notes a similarity between the observed features and those that Tandon & Leibovich (1995a) found in flow simulations but suggests that the vacillations in Lc's intensity may be a consequence of the downward motions inhibited by the buoyancy of subsurface bubble clouds. However, Farmer et al. (2001) use measurements of bubble void fraction, v_f, collected in 14 ms^{-1} winds to compare the magnitude of the torque term in Equation 2 induced by the Stokes drift, $(du_s/dz)(\partial u/\partial y)$, $\sim 4S_0\beta\Delta u/\Delta y$, with that of the bubble-induced buoyancy, $g\partial\rho/\partial y$, $\sim g\Delta v_f/\Delta y$. Δu is the difference in the downwind drift in and between the cells, Δy is the cell width, and Δv_f is the difference of the bubble void fraction across cells. Using Equations 5 and 6, and taking Δu to be $(0.01–0.02)W_{10}$ (the same order of magnitude as the Stokes drift), the ratio is $(320 \pm 110)\Delta v_f$—small because Δv_f is at most about 8×10^{-6}. Therefore, at these wind speeds, bubbles have an insignificant effect on Lc, refuting Smith's suggestion.

Plueddemann et al. (1996) and Plueddemann & Weller (1999) describe how, after an abrupt fall in wind speed, Lc persisted and maintained unstratified conditions in the upper 25 m for 24 h, even under daytime heating. The circulation was sustained by the more gradually decreasing wave field. Though seemingly consistent, the relation of these observations to Phillips' (2002) findings of a lower threshold for Lc onset in decaying waves is yet to be established.

Internal Waves and Lc

Evidence for a connection between Lc and internal waves is fragmentary. Perhaps the strongest comes from Farmer et al.'s (2001) measurements of acoustically detected bubble clouds and high-resolution temperatures in a storm with winds of about 14 ms^{-1}. Records show that temperature minima associated with the

deeper-going bubble clouds, and hence to Lc in the mixed layer, are linked in phase to temperature fluctuations within the thermocline.

This is an important aspect of Lc that deserves further investigation. Although it has long been speculated that mixed layer turbulence generates internal waves, little is known of the processes involved.

Turbulence and Bubble Clouds in Lc

Observations made at depths of (1.6–16) Hs, where Hs is the significant wave height, find that the mean rate of turbulent kinetic energy dissipation, ε, is enhanced by factors of two or more within the bands of bubble formed by Lc (Thorpe et al. 2003a,b). Bubble clouds and turbulence resulting from breaking waves are advected by the converging pattern of Lc and then subducted in the downwelling zones. However, the relative contributions to the local turbulence of advection from the highly turbulent near-surface region and that of turbulence enhancement by Lc (e.g., by vortex stretching) are presently unknown.

7. CONSEQUENCES OF LANGMUIR CIRCULATION

Mixed Layer Deepening

Although definitive observations are lacking, it appears that Lc erodes stratification by a process of engulfment (Li & Garrett 1995), in which colder fluid is advected vertically and carried over warmer. The resulting statically unstable stratification contributes to the mixing and homogenization of the temperature field within a near-surface mixed layer (see Section 4). Lc may locally enhance the shear at the base of the mixed layer, particularly where the downwind and descending flow below the surface convergences impinges on the thermocline, promoting shear instability and thermocline erosion.

Doubt remains about the real importance of Lc in mixed layer deepening. Weller & Price (1988) conclude that there is no evidence that Lc has a direct role in mixing near the base of a 40–60-m deep mixed layer (see also Figure 8). In the regions of downward flow in Lc in the depth range $1.5 < z/Hs < 12$, Thorpe et al. (2003a) find no evidence of the enhanced presence of temperature ramps produced by shear-induced eddies, as might be expected if the shear there is increased. Skyllingstad et al. (1999) compare LES simulations and observations during a 24-h period in fairly steady winds of about 12 ms^{-1} that includes nocturnal cooling with |L| exceeding 20 m. Except in the upper 10 m, where observations are not available because of the effect of the ship's wake, the comparison of model and measured values of ε and χ (the rate of temperature dissipation) in the mixed layer is satisfactory, although the measured ε increases more rapidly towards the surface than the model estimates. The model indicates that Lc is the dominant process controlling both ε and χ (the rate of temperature dissipation) in the upper 10 m, but at greater depths in the nocturnal mixed layer (extending to

40–60 m), eddies generated by shear and buoyancy dominate. In an LES study of the generation of inertial waves by a resonant wind field, Skyllingstad et al. (2000) conclude that the effects of Lc are mostly confined to the initial stages of mixed layer growth.

Dispersion of Buoyant Material, Bubbles, Oil, and Algae

Concentration of buoyant particles, oil droplets, or bubbles within Lc [in part a consequence of the process of trapping described by Stommel (1949)], and horizontal Lagrangian dispersion have been simulated using the LES models referred to in Section 5 (see also Figure 7). Thorpe et al. (1994) and Li (2000) devised models of dispersion in which particle motion is simulated by forcing it to conform to the varying location of bubble bands measured from sonar images. Li finds that generally across-wind diffusion exceeds downwind. Particles spend less time in Langmuir bands when they move downwind than when moving between them.

Precise estimates of even the rise speed of bubbles, important in modeling their vertical dispersion and contribution to air-sea gas flux, requires more information about the nature of enhanced turbulence within the downwelling regions of Lc where bubbles accumulate and where still-water bubble rise speeds are comparable to the turbulent velocity fluctuations (Thorpe et al. 2003b).

Deleterious Effects on Algae

It has been known for many years that Lc causes increased concentrations of motile or buoyant algae (e.g., see Bainbridge 1957, George 1981, Smayda & Reynolds 2001) (Figure 3). Dyke & Barstow (1983) describe Lc's importance to the ecology of the mixed layer by enhancing mixing, transporting organisms between high and low light levels, promoting patchiness of swimming or buoyant algae, or affecting their exposure to pollution. The increased levels of turbulence in the downwelling regions of Lc affect the supply of nutrients to algae, may increase predator-prey contact, and damage flagellates (for a review of the effects of turbulence on algae see Estrada & Berdalet 1998). Turbulent shear is near the threshold at which mechanical damage occurs to flagellates and at which negative effects on nitrogenase activity (NA) and CO_2 fixation by *Nodularia* strains of cyanobacteria occur (Thorpe et al. 2003b).

Other Processes

Other phenomena promote convergence or divergence at the sea surface and may so rapidly distort the surface flow that Lc is neither apparent nor effective in promoting dispersion. During strong tidal flows in shallow well-mixed seas, turbulent eddies can reach the surface from their source at the seabed, producing "boils" (Nimmo Smith et al. 1999). Thorpe (2001) discusses their competition with Lc in promoting dispersion. Estimates suggest that, in water 45-m deep, a transition

from domination by tidal eddies to Lc occurs when $W_{10}/U \approx 15$, where U is the tidal current speed.

8. CONCLUSION

Lc is an important process of transfer in the upper ocean. LES models are generally successful in replicating the observed features, and their predictions of Lc's 3D structure demand observational verification. At several points in this review we see that information is still lacking. Where it is perhaps most required is in the nature and variability of small-scale turbulence near the sea surface, frequently represented in models by an eddy viscosity, ν_T. For many processes associated with Lc (e.g., the dispersion of floating material), the near-surface region is critical and the very place where LES model accuracy is most in doubt because of turbulence and vorticity produced by breaking waves. This carries the subject beyond that of simply waves, wind, and heat or buoyancy flux and into the nature of turbulent motion and dissipation near the water surface or into unraveling processes that accompany the breaking of surface waves. This is an area of considerable complexity but one presently receiving attention. Breakers produce small-scale (<about 1 m) turbulence. If they also generate larger scale (1–20 m) horizontal vorticity, seeding Lc (Csanady 1994, Teixeira & Belcher 2002), the vorticity cascade to even larger scales suggested by the existence of a hierarchy of cell sizes will depend on the parameters that determine the statistical properties of breaking waves. Factors other than the Stokes drift and friction velocity determine the frequency of wave breaking and the associated momentum flux (Gemmrich & Farmer 1999, Melville & Matusov 2002) and, by establishing the input and scale of vorticity at the ocean surface, may consequently determine the form, the mean spacing of cells, and the circulation strength of Lc. The nature of cell hierarchy is relatively unexplored. Whether cells are superimposed or coexist separately alongside one another determines how effective they are in vertical dispersion (Thorpe et al. 2003b). May small cells be carried below the sea surface by larger cells, so contributing to subsurface turbulence? Is turbulence more intense in the vicinity of Y junctions and, if so, do Y junctions play a disproportionately large role in energy dissipation, mixing, or internal wave generation? The processes of vorticity generation and evolution need to be identified and quantified before Lc in the ocean can be understood.

Evidence that Lc dominates the vertical motions over some range of depth scales is still not entirely conclusive, nor is it known to what extent they affect the deepening of the mixed layer when its depth exceeds a few times the significant wave height. Nevertheless, the interaction between the flow field and motion of nonneutral particles, particularly bubbles and buoyant algae, leads to particle concentrations and implies that, for these particles, Lc is a very effective transport process. Presently lacking are measurements of statistical connections between the transient velocity, vorticity, and turbulence fields.

As is evident from the numerous papers that continue to be published, Lc is still a subject of great interest and fascination. Authors of existing LES models make and justify the claim that the effects of Lc are important enough to be included in models of the ocean mixed layer and in Global Circulation Models (GCMs), although how the effects should be represented parametrically is not yet clear. In view of its role in dispersion, algal dynamics, air-sea flux of gases and hence in climate, Lc will continue to attract attention in the years ahead. This review is but a passing glimpse of knowledge of a fascinating and colorful phenomenon that is an integral part of the still poorly understood dynamics of the upper ocean boundary layer.

ACKNOWLEDGMENTS

I am most grateful to Professor C. Garrett for helpful comments on an early draft, and to those who have kindly provided figures for reproduction and given permission to do so.

The *Annual Review of Fluid Mechanics* is online at http://fluid.annualreviews.org

LITERATURE CITED

Bainbridge R. 1957. The size, shape and density of marine phytoplankton concentrations. *Cambridge Philos. Soc. Biol. Rev.* 32:91–115

Bhaskaran R, Leibovich S. 2002. Eulerian and Langranian Langmuir circulation patterns. *Phys. Fluids* 14:2557–71

Cox SM. 1997. Onset of Langmuir circulation when the shear flow and Stokes drift are not parallel. *Fluid Dyn. Res.* 19:149–67

Craik ADD, Leibovich S. 1976. A rational model for Langmuir circulations. *J. Fluid Mech.* 73:401–26

Crow SC. 1970. Stability theory for a pair of trailing vortices. *AIAA J.* 8:2172–79

Csanady GT. 1973. *Turbulent diffusion in the environment*. Boston: Reidel, Dordrecht. 248 pp.

Csanady GT. 1994. Vortex pair model of Langmuir circulation. *J. Mar. Res.* 52:559–81

Chini GP, Leibovich S. 2003a. Resonant Langmuir circulation-internal wave interaction. Part 1. Internal wave reflection. *J. Fluid Mech.* Submitted

Chini GP, Leibovich S. 2003b. Resonant Langmuir circulation-internal wave interaction. Part 2. Langmuir circulation instability. *J. Fluid Mech.* Submitted

D'Asaro EA. 2000. Simple suggestions for including vertical physics in oil spill models. *Spill Sci. Technol.* 6:209–11

D'Asaro EA. 2001. Turbulent vertical kinetic energy in the ocean mixed layer. *J. Phys. Oceanogr.* 31:3530–37

D'Asaro EA, Dairiki GT. 1997. Turbulence intensity measurements in a wind-driven mixed layer. *J. Phys. Oceanogr.* 27:2009–22

D'Asaro EA, Farmer DM, Osse JT, Dairiki GT. 1996. A Lagrangian float. *J. Atmos. Ocean. Technol.* 13:1230–46

Dimas AA, Fialkowski LT. 2000. Large-wave simulation (LWS) of free-surface flows developing weak spilling breaking waves. *J. Comput. Phys.* 159:172–96

Donelan MA, Longuet-Higgins MS, Turner JS. 1972. Periodicity in whitecaps. *Nature* 239:449–51

Dyke PPG, Barstow SF. 1983. The importance of Langmuir circulations to the ecology of the mixed layer. In *North Sea Dynamics*, pp. 486–97. Berlin: Sündermann/Lenz, Springer-Verlag

Estrada M, Berdalet E. 1998. Effects of turbulence on phytoplankton. In *Physiological Ecology of Harmful Algal Bloom*, ed. DM Anderson, AD Cambella, GM Hallegraeff. *NATO ASI Ser.* G41:601–18

Etling D, Brown RA. 1993. Roll vortices in the planetary boundary layer: a review. *Bound. Meteorol.* 65:215–48

Faller AJ. 1964. The angle of windrows in the ocean. *Tellus* 16:363–70

Faller AJ, Caponi EA. 1978. Laboratory studies of wind-driven Langmuir circulation. *J. Geophys. Res.* 83:3617–33

Farmer DM, Li M. 1995. Patterns of bubble clouds organised by Langmuir circulation. *J. Phys. Oceanogr.* 25:1425–40

Farmer DM, Vagel S, Li M. 2001. Bubble and temperature fields in Langmuir circulations. In *Fluid Mechanics and the Environment: Dynamical Approaches*, ed. JL Lumley, pp. 95–105. New York: Springer

George DG. 1981. Zooplancton patchiness. *Rep. Freshwater Biol. Ass.* 49:32–44

Gemmrich JR, Farmer DM. 1999. Observations of the scale and occurrence of breaking surface waves. *J. Phys. Oceanogr.* 29:2595–606

Gnanadesikan A. 1996. Mixing driven by vertically variable forcing: an application to the case of Langmuir circulation. *J. Fluid Mech.* 322:81–107

Gnanadesikan A, Weller RA. 1995. Structure and instability of the Ekman spiral in the presence of surface gravity waves. *J. Phys. Oceanogr.* 25:3148–71

Handler RA, Smith GB, Leighton RI. 2001. The thermal structure of an air-water interface at low wind speeds. *Tellus* 53A:233–44

Huang NE. 1979. On surface drift currents in the ocean. *J. Fluid Mech.* 91:191–208

Kenney BC. 1993. Observations of coherent bands of algae in a surface shear layer. *Limnol. Oceanogr.* 38:1059–67

Langmuir I. 1938. Surface motion of water induced by wind. *Science* 87:119–23

Leibovich S. 1977. On the evolution of the system of wind drift currents and Langmuir circulations in the ocean. Part 1. Theory and averaged current. *J. Fluid Mech.* 79:715–43

Leibovich S. 1983. The form and dynamics of Langmuir circulations. *Annu. Rev. Fluid Mech.* 15:391–427

Leibovich S, Paolucci S. 1981. The instability of the ocean to Langmuir circulations. *J. Fluid Mech.* 102:141–67

Li M. 2000. Estimating horizontal dispersion of floating particles in wind-driven upper ocean. *Spill Sci. Technol.* 6:255–62

Li M, Garrett C. 1993. Cell merging and the jet/downwelling ratio in Langmuir circulation. *J. Mar. Res.* 51:737–96

Li M, Garrett C. 1995. Is Langmuir circulation driven by surface waves or surface cooling? *J. Phys. Oceanogr.* 25:64–76

Li M, Garrett C. 1997. Mixed-layer deepening due to Langmuir circulation. *J. Phys. Oceanogr.* 27:121–32

Li M, Zahariev K, Garrett C. 1995. The role of Langmuir circulation in the deepening of the ocean surface mixed layer. *Science* 270:1955–57

McIntyre ME. 1981. On the "wave-momentum" myth. *J. Fluid Mech.* 106:331–47

McWilliams JC, Sullivan PP. 2000. Vertical mixing by Langmuir circulations. *Spill Sci. Technol. Bull.* 6:225–38

McWilliams JC, Sullivan PP, Moeng C-H. 1997. Langmuir turbulence in the ocean. *J. Fluid Mech.* 334:31–58

Melville WK, Matusov P. 2002. Distribution of breaking waves at the sea surface. *Nature* 417:58–63

Nimmo Smith WAM, Thorpe SA, Graham A. 1999. Surface effects of bottom-generated turbulence in a shallow tidal sea. *Nature* 400:251–54

Phillips WRC. 2001. On an instability to Langmuir circulations and the role of Prandtl and Richardson numbers. *J. Fluid Mech.* 442:335–58

Phillips WRC. 2002. Langmuir circulations beneath growing or decaying surface waves. *J. Fluid Mech.* 469:317–42

Plueddemann AJ, Smith JA, Farmer DM, Weller RA, Crawford WR, et al. 1996.

Structure and variability of Langmuir circulation during Surface Waves Processes Program. *J. Geophys. Res.* 101:3525–43

Plueddemann AJ, Weller RA. 1999. Structure and evolution of the oceanic surface boundary layer during the Surface Waves Processes Program. *J. Mar. Res.* 21:85–101

Polonichko V. 1997. Generation of Langmuir circulation for nonaligned wind stress and the Stokes drift. *J. Geophys. Res.* 102:15,773–80

Pollard RT. 1977. Observations and theories of Langmuir circulations and their role in near surface mixing. In *A Voyage of Discovery: George Deacon 70th Anniversary Volume*, ed. M Angel, pp. 235–51. Oxford: Pergamon

Price JF, Weller RA, Pinkel R. 1986. Diurnal cycling. Observations and models of the upper ocean response to diurnal heating, cooling and wind mixing. *J. Geophys. Res.* 91:8411–27

Rieder KF, Smith JA. 1994. Removing wave effects from the wind stress vector. *J. Geophys. Res.* 103:1363–74

Skyllingstad ED, Denbo DW. 1995. An ocean large-eddy simulation of Langmuir circulations and convection in the surface mixed layer. *J. Geophys. Res.* 100:8501–22

Skyllingstad ED, Smyth WD, Crawford GB 2000. Resonant wind-driven mixing in the ocean boundary layer. *J. Phys. Oceanogr.* 30:1866–90

Skyllingstad ED, Smyth WD, Moum JN, Wijesekera H. 1999. Upper-ocean turbulence during a westerly wind burst: a comparison of large-eddy simulation results and microstructure measurements. *J. Phys. Oceanogr.* 29:5–28

Smayda TJ, Reynolds CS. 2001. Community assembly in marine phytoplankton; applications of recent models to harmful dinoflagellate blooms. *J. Plankton Res.* 23:447–61

Smith JA. 1992. Observed growth of Langmuir circulation. *J. Geophys. Res.* 97:5651–64

Smith JA. 1996. Observations of Langmuir circulation, waves and the mixed layer. In *The Air-Sea Interface: Radio and Acoustic Sensing, Turbulence and Wave Dynamics*, ed. MA Donelan, WH Hi, WJ Plant, pp. 613–22. Univ. Toronto Press

Smith JA. 1998. Evolution of Langmuir circulation during a storm. *J. Geophys. Res.* 103:12,649–68

Smith J, Pinkel R, Weller RA. 1987. Velocity structure in the mixed layer during MILDEX. *J. Phys. Oceanogr.* 17:425–39

Stommel H. 1949. Trajectories of small bodies sinking slowly through convection cells. *J. Mar. Res.* 8:24–29

Tandon A, Leibovich S. 1995a. Simulations of three-dimensional Langmuir circulation in water of constant density. *J. Geophys. Res.* 100:22,613–23

Tandon A, Leibovich S. 1995b. Secondary instabilities in Langmuir circulations. *J. Phys. Oceanogr.* 25:1206–17

Teixeira MAC, Belcher SE. 2002. On the distribution of turbulence by a progressive surface wave. *J. Fluid Mech.* 458:229–67

Thorpe SA. 1992. The break-up of Langmuir circulation and the instability of an array of vortices. *J. Phys. Oceanogr.* 22:350–60

Thorpe SA. 1997. Interactions between internal waves and boundary layer vortices. *J. Phys. Oceanogr.* 27:62–71

Thorpe SA. 2001. Langmuir circulation and the dispersion of oil spills in shallow seas. *Spill Sci. Technol. Bull.* 6:213–24

Thorpe SA, Curé MS, Graham A, Hall AJ. 1994. Sonar observations of Langmuir circulation and estimation of dispersion of floating bodies. *J. Atmos. Ocean. Technol.* 11:1273–94

Thorpe SA, Osborn TR, Jackson JFE, Hall AJ, Lueck RG. 2003a. Measurements of turbulence in the upper ocean mixing layer using Autosub. *J. Phys. Oceanogr.* 33:122–45

Thorpe SA, Osborn TR, Farmer DM, Vagel S. 2003b. Bubble clouds and Langmuir circulation: observations and models. *J. Phys. Oceanogr.* 33:2013–31

Veron F, Melville WK. 2001. Experiments

on the stability and transition of wind-driven water surfaces. *J. Fluid Mech.* 446:25–66

Weller RA, Price JF. 1988. Langmuir circulation within the oceanic mixed layer. *Deep-Sea Res.* 35:711–47

Weller RA, Dean JP, Marra J, Price JF, Francis EA, Broadman DC. 1985. Three-dimensional flow in the upper ocean. *Science* 227:1552–56

Zedel L, Farmer D. 1991. Organised structures in subsurface bubble clouds: Langmuir circulation in the open ocean. *J. Geophys. Res.* 96:8889–900

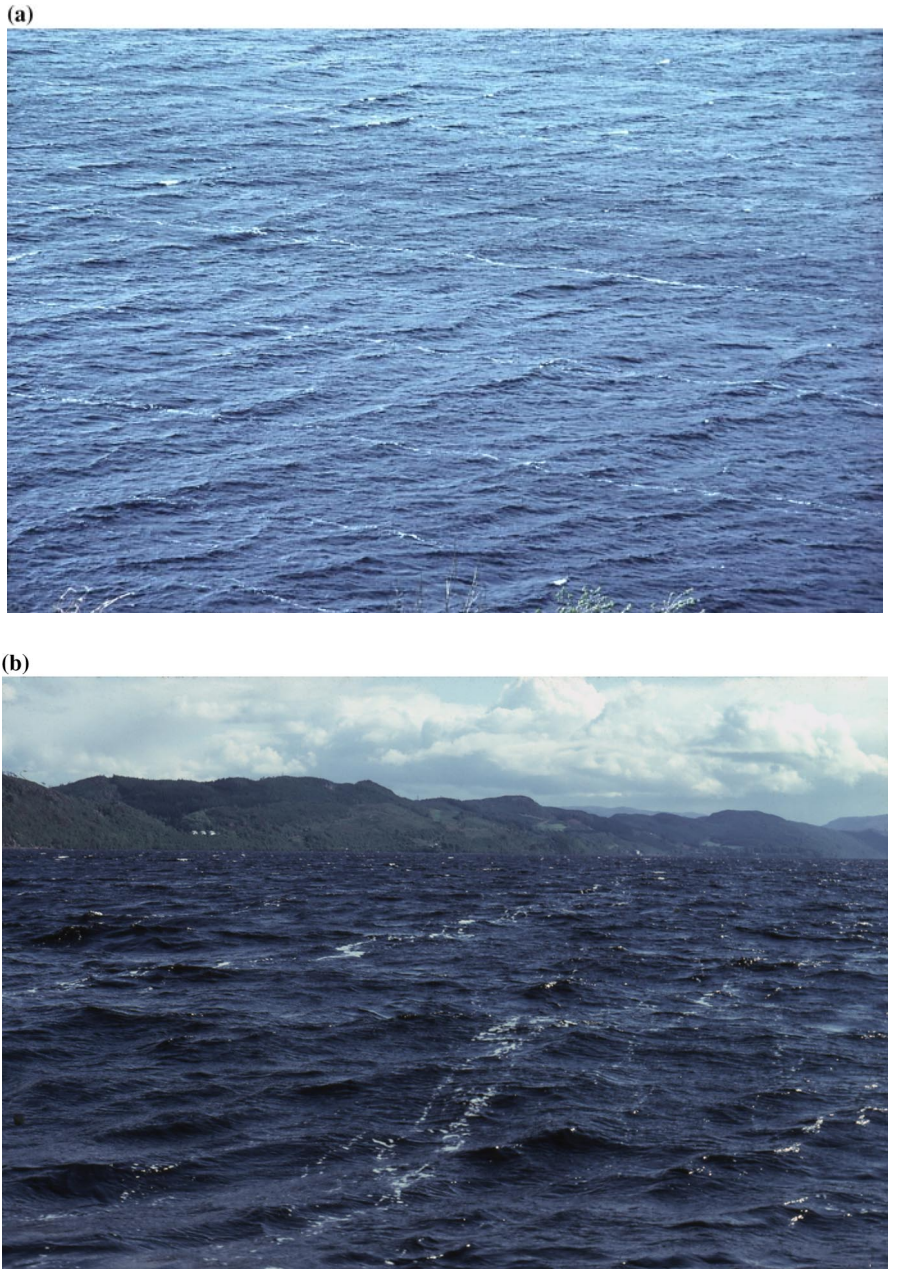

Figure 2 Windrows comprised mainly of foam from breaking waves marking the surface convergence regions of Langmuir circulation in the fresh-water lake, Loch Ness. Their spacing is about 10 m. Views are (*a*) obliquely from above, and (*b*) from close to the surface of the loch.

Figure 3 Subsurface bands of toxic algae observed in the German Bight of the North Sea in August 1988, a few meters apart. The splash at bottom left is part of the ship's bow wave. (Photo kindly provided by Dr. M. Blackley.)

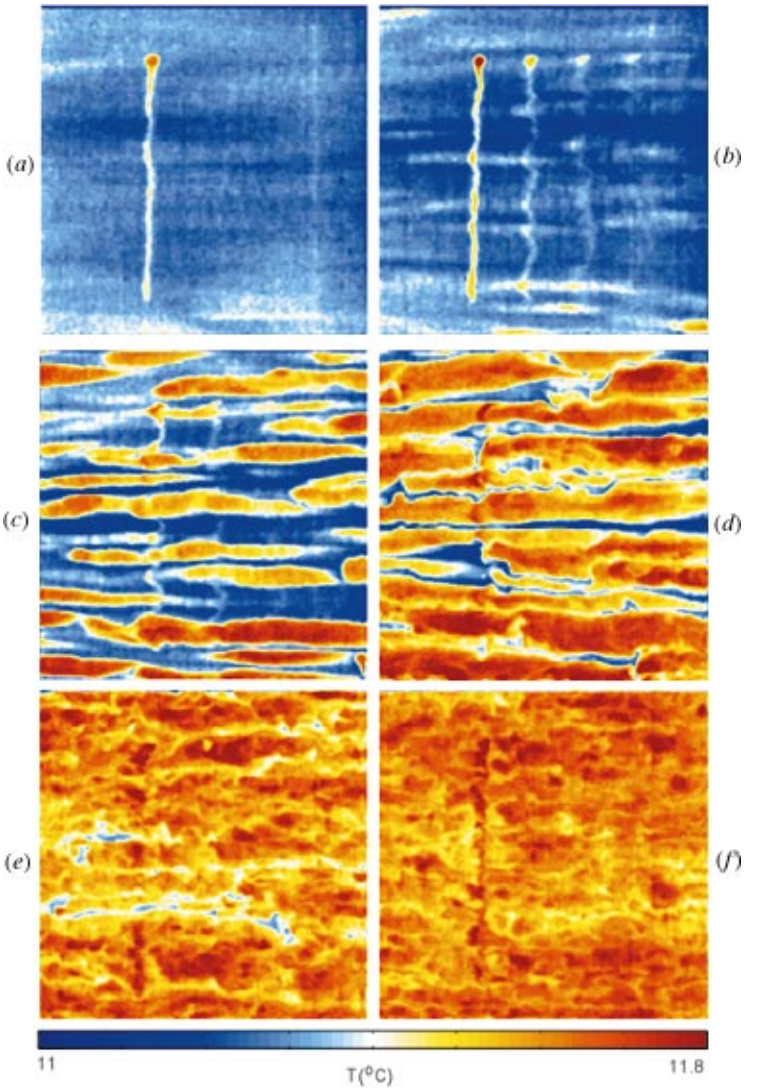

Figure 6 Small-scale Langmuir cells visible in the surface temperature field formed shortly after the onset of a 5 ms^{-1} wind in laboratory experiments. Times of a–f are 16.8, 18.3, 19.8, 21.3, 22.8, and 24.3 s, respectively, after the onset of wind, and the image width is 0.4 m. The vertical wavy lines are thermal markers laid down by a laser. Temperature is in °C. There is a transition to a small-scale irregular flow in f. (From Veron & Melville 2001 with kind permission of Cambridge Univ. Press.)

Annual Review of Fluid Mechanics
Volume 36, 2004

CONTENTS